NEW TECHNOLOGIES OF PRODUCTION AND PROCESSING OF MATERIALS

TiC−Cr₃C₂−WC−NiCr−Mo−C Cermet Plasma Coatings

V. I. Kalita[a], *, A. A. Radyuk[a], **, D. I. Komlev[a], A. B. Mikhailova[a], ***, A. V. Alpatov[a], ****, and D. D. Titov[a], *****

[a] Baikov Institute of Metallurgy and Materials Science, Russian Academy of Sciences, Moscow, 119334 Russia
*e-mail: vkalita@imet.ac.ru
**e-mail: imet-lab25@yandex.ru
***e-mail: sasham1@mail.ru
****e-mail: alpat72@mail.ru
*****e-mail: mitytitov@gmail.com

Abstract—Two bulk cermets TiC−WC−Cr₃C₂−(Ni80Cr20)−Mo−2.8C after liquid-phase sintering at 1400°C for 1 h were used to manufacture powders for plasma spraying of coatings. The cermets were fabricated at a limited time of mechanical alloying at the mixing stage. Plasma coatings were sprayed on a setup with a nozzle attached to a plasmatron for local protection of the sprayed particles from the air atmosphere. The WC−Cr₃C₂−C content in the cermets provided compensation for carbon losses at all stages of coating production and the formation of an annular zone, the volume of which determines the increase in the TiC content in the coatings by 20% and the formation of additional carbides in the matrix. The microhardness of cermet at an initial carbide content of 60% was 15.26−16.83 GPa with a load on the indenter of 200 G and 20.91−24.68 GPa with a load on the indenter of 20 G, and the difference was explained by a scale factor. The contribution of the microhardness of carbides to the microhardness of cermet with an initial carbide content of 60% was estimated according to the rule of mixtures, proceeding from their volume fraction and microhardness of cermet under a load on the indenter of 20 G. In the initial powder for spraying, this contribution is high, 33.19 GPa, close to the hardness of TiC. The contribution of microhardness of carbides in the coating is lower, 28.09 GPa.

Keywords: plasma spraying, coating, cermet, TiC−WC−Cr₃C₂−C, nozzle to the plasmatron, carbon loss, calculation of microhardness of carbides

DOI: 10.1134/S2075113321050178

INTRODUCTION

Gas-thermal TiC-based cermet coatings are promising and can compete with WC−Co, since they operate at higher temperatures, have a higher hardness, and dissolve less in the matrix phase during plasma spraying [1−7]. Despite this, there are not many publications on these cermet coatings [2−7]. A much larger number of publications are devoted to bulk cermets fabricated by liquid-phase sintering at temperatures of 1300−1500°C [8−21]. In the latter publications on bulk cermets, special attention is paid to increasing their mechanical properties (transverse strength, hardness, and crack resistance) through to the formation of a strong bond between TiC and the matrix. This is implemented when cermets are alloyed with additional Mo₂C, WC, Cr₃C₂ carbides, which form an annular zone, which is better wetted by the liquid matrix phase, is more plastic than TiC, and at the same time has a high hardness with limited thickness [11]. The introduction of additional carbon is used to counteract oxygen, the content of which

reaches 4 wt % after mechanical alloying (MA) [21]. A supplementary addition of carbon up to 3 wt % to compensate for its losses at the MA and plasma spraying stage was used in recent studies on plasma TiC-based cermet coatings [1, 22].

Annular zones are more difficult to fabricate at a short residence time of the sprayed particle in the plasma jet. WC and Cr₃C₂ carbides have lower formation energy, and it is possible to assume their preferential dissolution in a liquid matrix during plasma spraying in comparison with TiC. In this case, carbon of these carbides interacts more with residual oxygen, while maintaining the content, stoichiometry, and hardness of the main TiC carbide, which makes it possible to conventionally call WC and Cr₃C₂ "sacrificial" carbides.

The purpose of this work is to optimize the composition and structure of the sprayed cermet powder by introducing additional carbides and carbon into the initial composition, as well as by using liquid-phase sintering, in which it is possible to prepare a dense structure

and the desired phase composition, including the formation of annular zones around TiC carbides.

MATERIALS AND METHODS

Two compositions of cermets differing in the total content of the initial carbides (60 and 80 wt %) were studied in this work. The initial mixtures had the following compositions (wt %): composition 1: 45% TiC–5% WC–10% Cr$_3$C$_2$–26.2% (Ni–20% Cr)–11% Mo–2.8% C; composition 2: 65% TiC–5% WC–10% Cr$_3$C$_2$–12.2% (Ni–20% Cr)–5% Mo–2.8% C. The content of the matrix phase in cermet 2 is less than that in cermet 1, including the Mo content, although the ratio between Ni–20% Cr and Mo is preserved. Additional carbon in the amount of 2.8% was introduced into the initial compositions of cermets in the form of soot, taking into account its losses at the stages of the powder production and during spraying, which was determined in previous studies. To reduce carbon losses and reduce the oxygen content when mixing the initial mixture, the MA time in a planetary mill was limited to 10 min; the process was carried out in an atmosphere of highly pure nitrogen with threefold preliminary blowing of the bowls. Carbide powders from the Donetsk Khimreaktivov Plant had an average particle size of 4 μm, and the average size of carbides decreased to 2 μm after MA. The resulting mixture of powders was pressed at room temperature at a specific pressure of 30 kg/mm^2, and a compact was sintered in vacuum at a temperature of 1400°C for 1 h. The cake was ground into powder for spraying, which was scattered on sieves to obtain a fraction of 32–71 μm. The coatings were sprayed on a UPU-3D universal plasma facility with a standard PP-25 plasmatron with an anode nozzle diameter of 6 mm. The plasmatron (plasma jet) power was increased by increasing the nitrogen content in argon (Table 1). The coating samples were marked as follows: the first digit is the number of the powder, the second digit after the period is the number of the spraying mode (Table 1). A water-cooled nozzle to the plasmatron with a length equal to the deposition distance of 170 mm was used for the local protection of the sprayed powder from the air atmosphere. The nozzle was developed at the Baikov Institute of Metallurgy and Materials Science, Russian Academy of Sciences, and is described in detail in [23]. The usefulness of such a nozzle lies in the extraction of the plasma flow after heating and the acceleration of the sprayed particles. The plasma-forming gas returns to the coating formation zone after cooling and cleaning in order to maintain an inert atmosphere. When using a nozzle, the oxygen content in the spraying zone is reduced by a factor of 20 compared to spraying with an open jet. The hot inner walls of the nozzle, the temperature of which reaches 1500°C, make it possible to reduce the temperature gradient of the plasma flow and the sprayed particles along the radius of the spray spot and increase the heat

transfer from the plasma to the sprayed particles (the required effective the power of the plasma jet is reduced by a factor of 2), which ultimately makes it possible to form a more uniform structure of the coating. Spraying was carried out at voltages in the arc of the plasmatron of 50, 55, 60 and 67 V, the current strength was constant (350 A), and the total plasma gas flow rate was 36.5 L/min (Table 1). The arc voltage was changed by adding nitrogen to the main plasma-forming gas, argon. The powder was fed into the plasmatron at a flow rate of 16.3 g/min from a tray powder feeder with an Ar carrier gas at a flow rate of 3.5 L/min through a hole in the anode with a diameter of 2 mm at a distance of 9 mm from its outlet end. For X-ray studies, 0.3 mm thick coatings were sprayed onto a 1-mm-thick moving steel substrate. Microsections were fabricated of powders and coatings in order to determine the microhardness and to carry out metallographic studies using optical microscopy—coatings up to 1 mm thick were sprayed onto steel substrate 5 mm thick. In order to increase the adhesion and cohesive properties of the coating, by improving the process of chemical interaction (wetting) between the molten particles and the sprayed surface, an additional spraying was carried out on a substrate preheated to 400°C. In the experiments, the powder utilization factor (PUF) was determined—the percentage of the powder that formed the coating.

The carbon content in the powder and coating was determined using CS-600 equipment (LECO) by oxidative melting of the powder in a ceramic crucible and subsequent measurement of the carbon content in gaseous CO$_2$ by infrared absorption, and the oxygen and nitrogen content was determined by reduction melting on a TC-600 analyzer (LECO) after the interaction of molten samples with the material of graphite crucibles and subsequent analysis of the released N$_2$ and CO or CO$_2$. The standard deviation of the mean did not exceed 1% for carbon, 4% for oxygen, and 6% for nitrogen.

The microhardness of powders and coatings made of them was determined on microsections of their cross sections by seven measurements on a PMT-3 facility at loads on the indenter of 20 and 200 G. The indentation from the indenter when measuring the microhardness under a load of 200 G covers several sprayed particles and the pore space between them, which characterizes the integral microhardness of the coating, taking into account the effect of porosity and the level of cohesion. When measuring the microhardness with a load of 20 G, an indentation with an indenter is carried out in the middle of the section of a single particle. This characterizes the microhardness of the sprayed material to a greater extent, which is important for establishing the relationship between the phase composition of the coating and its microhardness. It should be noted that, even at a load of 20 G, the diagonal of the indentation is approximately equal to the average thickness of a single deposited particle,

Table 1. Dependence of the phase composition of powders for spraying and coatings deposited from these powders on the plasmatron power during spraying

Sample no.	Plasmatron power, kW	Plasma power, kW	Phase content, wt %;							TiC lattice period, nm
			TiC	CrNi	$CrNi_3$	$Cr_{0.8}Ni_{0.2}$	Cr_7C_3	Cr_3C_2	Σ of carbides	
1	−		58.7	−	25.8	−	13.5	2	74.2	0.4307
1.1	17.2	8.4	68.1	−	20.5	2.3	3.1	5.6	76.8	0.4307
1.2	18.9	10.2	72.4	18.8	−	2.1	4.7	2	79.1	0.4305
1.3	21	12.6	74.1	19.4	−	2.1	1.3	3.1	78.5	0.4306
1.4t*	21	12.6	72.9	−	19.9	2.8	3.3	1.1	77.3	0.4303
1.5	26.8	18.0	72.3	18.9	−	2.6	3.3	2.9	78.5	0.4306
2	−	−	80.8	−	8.2	4	6.3	0.7	87.8	0.4308
2.1	17.5	8.8	78.7	−	13.6	3.7	2.4	1.6	82.7	0.4308
2.2	19.25	9.6	76.8	−	13.8	3.9	3.6	1.9	82.3	0.4305
2.3	21	12.6	75.9	−	14.9	3.2	3.1	2.9	81.9	0.4306
2.4t*	21	12.6	81.4	−	13.2	2.9	1.3	1	83.7	0.4308
2.5	26.8	18	82.1	−	12.9	2.1	1.3	0.9	84.3	0.4303

*t** − spraying was carried out on a substrate heated to 400°C.

and the effect of pores on the boundaries between particles reduces the actual microhardness. If the rules for measuring microhardness were observed, the indentation should have been five times less than the thickness of the particles, that is, approximately 1 μm.

RESULTS

When analyzing the structure of cermets after liquid-phase sintering and plasma spraying, it was assumed that titanium carbide only partially dissolves in the liquid matrix phase [21]. Carbides in powders for spraying are distributed relatively evenly, and the matrix phase occupies the space between carbides (Fig. 1). The higher chipping of the carbide phase in powder 2 and the coating from it during the manufacture of the microsection is apparently determined by the lower content of the matrix phase, which plays the role of a binding element (Fig. 2). Chipping of the car-

bide phase in the coating decreases in the coatings of both compositions with the increase in the plasmatron power (Fig. 2). When the plasmatron power increases, the contrast between the carbide and matrix phases decreases, apparently because of the higher dissolution of carbides in the matrix phase heated to higher temperatures and the subsequent formation of an annular zone around TiC with a gradient change in the composition.

The calculated carbon content of 12.49 wt % in the initial mixture of composition 1 (the calculation used the data of analyses on the carbon content in the initial components of the cermet) in the coating decreased to 10.48 wt %; that is, the relative carbon content decreased by 16.1% (Table 2). In comparison with the powder for spraying (11.2 wt % C), the relative carbon content in the coating decreased by 6.4%. The average carbon content in the coatings of 0.79 wt % is higher
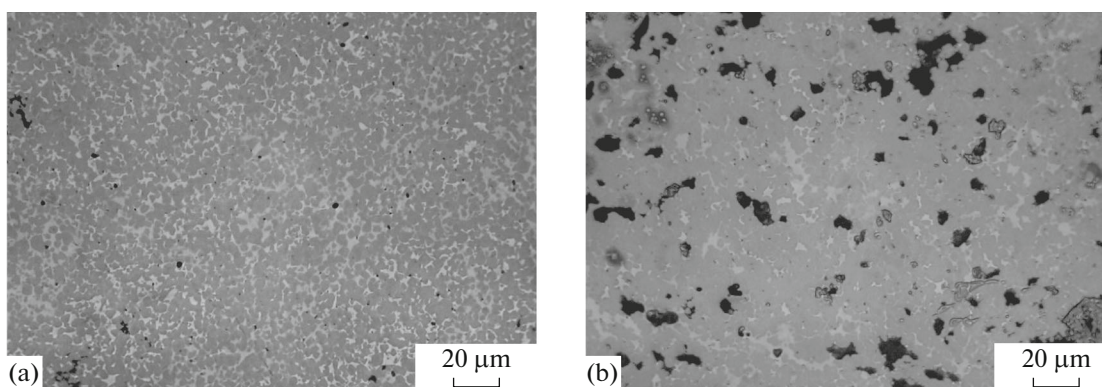

Fig. 1. Microstructure of cakes of compacts from powders of composition (a) 1 and (b) 2.
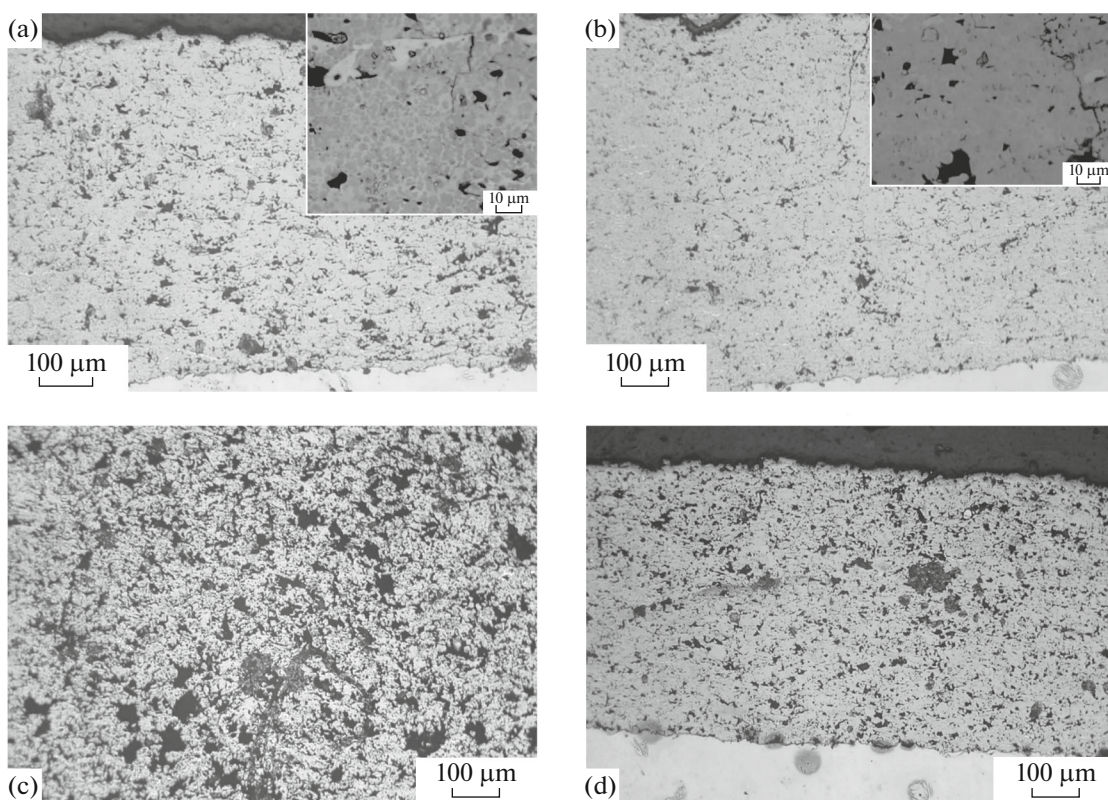
Fig. 2. Coatings of powder of composition 1 (a, b) and 2 (c, d) sprayed at an effective plasma jet power of (a, c) 8.4 and (b, d) 18 kW.

than that in the original carbides or 8.51% on a relative basis. This means that 2.01 wt % C out of 2.8 wt % C of additional carbon was consumed.

The calculated initial carbon content of 14.72 wt % in cermet 2 decreased to 14.16 wt % in the coating, that is, by 3.8% on a relative basis. In comparison with the powder for spraying (14.6 wt % C), the relative carbon content in the coating decreased by 3.01%. Cermet coatings 2 have on average 2.24 wt % more carbon than original carbides or 18.79% on a relative basis. This means that 0.56 wt % C out of 2.8 wt % C of additional carbon was consumed.

The X-ray analysis records 60 wt % of carbides in cermet 1 in the initial mixture, 74.2 wt % of carbides in the powder for spraying, and 78.04 wt % of carbides in the coating; in cermet 2, there are 80 wt % of carbides in the initial mixture, 87.8 wt % of carbides in the powder for spraying, and 82.98 wt % of carbides in the coating (Table 1). Such an increase in the carbide content is associated with the reaction of additional carbon with the Cr and Mo matrix already at the stage of liquid-phase sintering. Taking into account the content of 1.54 wt % of additional carbon in powder for spraying of cermet 1, the calculation indicates that Cr and Mo completely leave the matrix, forming 6 wt % of Cr$_3$C$_2$ and 11.7 wt % of Mo$_2$C owing to the reaction with this additional carbon, and as a result, 17.7 wt % of additional carbides are formed. We recorded 14.3 wt % of

additional carbides in the powder. An average of 0.78 wt % of additional carbon remains in the coating, but the carbide content is higher than that in the powder, which is explained by the formation of nonequilibrium carbides with a lower carbon content [23]. Some of the new carbides, together with the original WC and Cr$_3$C$_2$ carbides, form an annular zone around the TiC, while some of the carbides can be formed in the matrix when it solidifies. As early as at the stage of the liquid-phase sintering, no WC carbide is detected, W of which can enter the annular zone and the matrix. Similar changes take place for cermet 2, with the only difference that the TiC content increases to the maximum value as early as at the stage of liquid-phase sintering. Such a calculation of additional carbides based on additional carbon and matrix elements is formal; in reality, a fraction of carbon can remain in the matrix both in the form of nickel-based carbides and in the form of free carbon [23]. The content of carbides is 87.2 vol % in coating 1.2 of cermet 1 and 89.1 vol % in coating 2.2 of cermet 2.

The average value of the TiC lattice period for coatings made of powder of composition 1 is 0.4305 nm, which is lower than that of the powder for spraying of 0.4307 nm. The average value of the lattice period of TiC for coatings of composition 2 is 0.4306 nm, which is also lower than that in the powder for spraying of 0.4308 nm. Such changes can be associated with a

Table 2. Content of carbon, oxygen, and nitrogen in powders for spraying and coatings, wt %

Sample no.	C	O	N
Powder for spraying, composition 1	11.2	0.858	0.15
p1.1	10.6	1.43	0.29
p1.2	10.6	1.20	0.36
p1.3	10.5	1.17	0.42
p1.4.t	10.2	1.43	0.39
p1.5	10.5	1.42	0.48
Average values over coatings, composition 1	10.48	1.33	0.39
Relative change in coatings with respect to powder, %*	−6.4	+55.01	+260
Powder for spraying, composition 2	14.6	0.642	0.18
2.1	14.0	1.32	0.34
2.2	14.1	1.11	0.40
2.3	14.2	1.16	0.43
2.4.t	14.4	1.30	0.41
2.5	14.1	1.26	0.57
Average values over coatings, composition 2	14.16	1.23	0.43
Relative change in coatings with respect to powder, %**	−3.01	+91.59	+138.89

 * Calculated carbon content in initial carbides, 9,69%.
** Calculated carbon content in initial carbides, 11.92%.

change in the stoichiometric ratio of elements in TiC carbide and primarily in its outer layers, where the annular zone is formed. In the X-ray diffraction pattern of a sample of coating 1.4, the right-hand parts of the reflections for $TiC_x Me_{1-x}$ carbide are shifted; a broadening with a shift to the right of all reflections is noticeable, and this is especially noticeable at large angles and in the lower part of the peaks (Fig. 3). This effect can be explained by the formation of an annular zone around the unmolten part of the TiC carbide of the annular zone in the form of a carbide of a complex composition based on Ti, Mo, Cr, W, Ni, and C. The formation of these phases leads to the decrease in the period and the distortion of the lattice of the unmolten part of the TiC carbide because of the integral radiation from TiC and the annular zone. The Cr content of 20 wt % in TiCrC carbide reduces the lattice period to 0.4301 nm [17]. Ternary carbide based on 64.8 wt % TiC—22.8 wt % Cr_3C_2—12.4 wt % WC has a lattice period of 0.4250 nm at a high microhardness of 42.3 GPa [8]. The elements forming the annular zone can form nanosized carbides in the matrix or remain in its solid solution during its solidification at high cooling rates, and, as a consequence, the lattice period of the matrix phase in the coating increases, which was observed earlier [23].

N and O can participate in the formation of the annular zone, the content of which in the coating increases by almost two times in comparison with the powder for spraying. A somewhat larger TiC lattice period for coating 2 can be associated with a smaller volume of the liquid matrix phase, in which TiC and oxygen are dissolved.

For coatings made of powder of composition 1, the maximum hardness under a load on an indenter of 20 G is 24.7 GPa, which is lower than that of the initial powder for spraying (27.3 GPa), while for coatings of composition 2, these values are close—27.6 and 27.8 GPa (Table 3, Fig. 4); at a load on the indenter of 200 G for coatings made of powder of composition 1, the maximum hardness is 16.8 GPa, higher than that of powder (15.9 GPa), while for coatings made of pow-
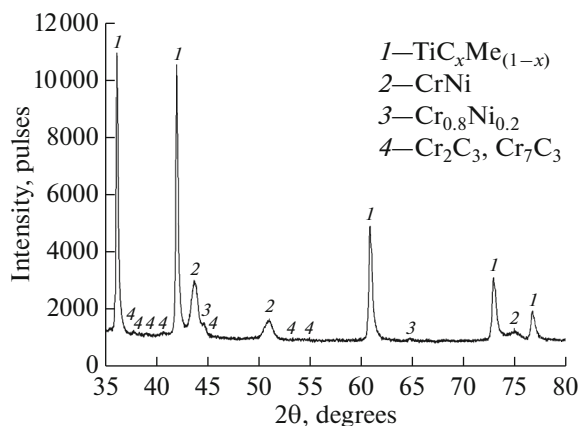

Fig. 3. X-ray diffraction pattern of the coating sample 1.4: (*1*) $TiC_x Me_{1-x}$, (*2*) nickel-based solid solution (CrNi), (*3*) chromium-based solid solution $Cr_{0.8}Ni_{0.2}$, (*4*) chromium carbides (Cr_2C_3, Cr_7C_3).

Table 3. Microhardness of powders for spraying and plasma coatings, GPa

Sample no.	Microhardness of samples (GPa) under load on the indenter, G	
	200	20
Powder, composition 1	15.9 ± 1.12	27.3 ± 4.42
1.1	15.3 ± 2.07	21.5 ± 4.96
1.2	15.3 ± 1.30	24.7 ± 3.38
1.3	16.1 ± 0.98	23.4 ± 3.00
1.4t*	16.8 ± 2.01	20.9 ± 2.90
1.5	16.8 ± 1.46	24.2 ± 2.95
Powder, composition 2	20.2 ± 2.08	27.8 ± 2.78
2.1	10.5 ± 2.01	26.8 ± 2.72
2.2	13.4 ± 1.52	27.6 ± 4.84
2.3	16.7 ± 2.64	24.7 ± 4.08
2.4t*	18.9 ± 1.84	26.0 ± 5.66
2.5	20.4 ± 2.33	23.2 ± 4.60

t* — spraying was carried out on a substrate heated to 400°C.

der composition 2, they again take close values—20.2 and 20.4 GPa. For all coatings, the microhardness at a load on the indenter of 20 G slightly decreases with the increase in the effective plasmatron power; these changes lie within the confidence interval (Fig. 4). The hardness of the coatings at this load is close to the hardness of the powder for spraying. The latter also refers to the hardness under a load on the indenter of 200 G, but for coatings of composition 2, this is observed at the maximum effective plasmatron power. Under a load of 200 G on the indenter, the hardness of coatings of composition 1 increases slightly with an increase in the effective plasmatron power from 15.3 to 16.8 GPa, and the hardness increases more intensely

for coatings of composition 2—from 10.5 to 20.4 GPa. Obviously, when spraying cermets of composition 2, it is necessary to heat the sprayed particles to higher temperatures for activation of the higher content of carbides, also for their synthesis from residual additional carbon. The more intense increase in the hardness at a load of 200 G as compared to the hardness at 20 G determines the increase in the H_{200}/H_{20} ratio at the increase in the effective plasma power. This can be explained by the decrease in the content of microstructure defects, decrease in porosity, and increase in the strength of the bond of the matrix and carbides. In this case, the hardness at the load of 20 G even decreases at the maximum plasma power, which can occur through the partial degradation of carbides.

DISCUSSION

The goal to preserve the total carbon content in cermets that was set in this study was achieved by introducing additional carbon into the composition of the initial mixture in the form of soot. A part of this carbon compensates for its losses during the reduction of oxides and neutralization of oxygen during deposition, a part forms an annular zone, and a part may remain in the matrix, strengthening it. We assume that new carbides, together with the initial "sacrificial" WC and Cr₃C₂ carbides, form an annular zone and therefore increase the TiC carbide content determined by X-ray phase analysis, both in powder for spraying and in coatings with a simultaneous decrease in the content of the matrix phase and additional carbon. In this study, we used WC and Cr₃C₂ carbides to form an annular zone, which together with Mo provide a strong bond between TiC and the matrix phase [11, 12, 16, 18]. A part of WC, Cr₃C₂, and Mo become components of the matrix, and during its solidification, they can form nanosized carbides and supersaturated solid
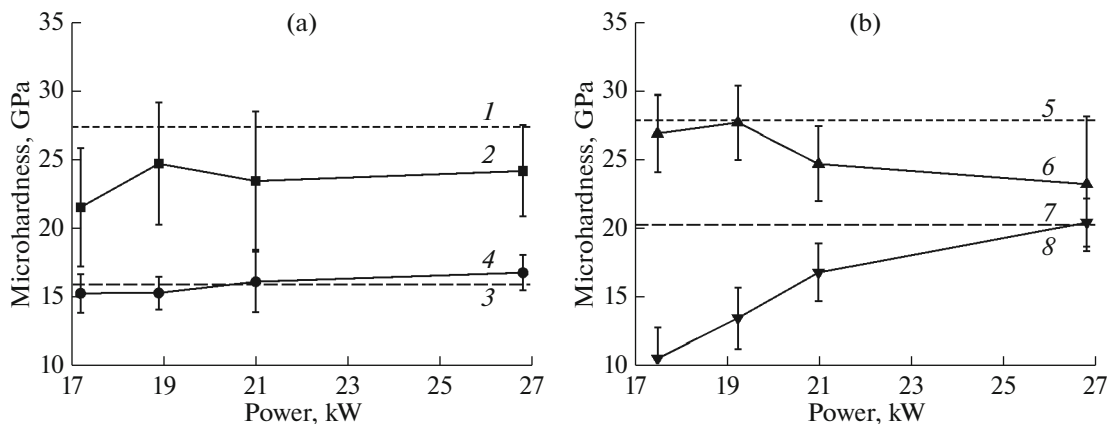

Fig. 4. Dependence of microhardness of coatings on the plasmatron power at loads on the indenter of 20 and 200 G: (a) (*1*) powder of composition 1, 20 G; (*2*) coatings of powder of composition 1, 20 G; (*3*) powder of composition 1, 200 G; (*4*) coatings of powder of composition 1, 200 G; (b) (*5*) powder of composition 2, 20 G; (*6*) coatings of powder of composition 2, 20 G; (*7*) powder of composition 2, 200 G; (*8*) coatings of powder of composition 2, 200 G.

Table 4. Volume fractions of carbides, U_{car}, vol %, and the calculated contribution of the hardness of carbides to the hardness of cermets, H_{car}, GPa, measured at a load of 20 G

Sample	Carbide content, U_{car}, vol %	Calculated contribution of the hardness of carbides to the hardness of cermets, H_{car}, %
Powder 1*	81.51	33.19
Coating 1.2	87.2	28.09
Powder 2	86.42	31.95
Coating 2.2	89.1	30.84

* Earlier, for a cake of a similar composition, at 84 vol % of carbides, their calculated hardness was 28.24 GPa [23].

solutions, strengthening the matrix phase during plasma spraying [1]. Works on elemental analysis of annular zones and matrix phase of TiC-based cermets are known [11, 12, 16, 18]. The positive effect of the introduction of $Mo_2C–WC–Cr_3C_2$ carbides is confirmed by the inclusion of these elements in the composition of the annular zones and the high mechanical properties of these cermets [11, 12, 16, 18]. These works served as a basis for the selection of the studied compositions in this study. In 46% TiC–11% Mo_2C–20% WC–5% TiN–10% Ni–8% Co cermet (all in wt %), the compositions of the inner annular zone (73.75% Ti–16.08% W–10.17% Mo), outer annular zone (80.2% Ti–10.91% W–8.84% Mo), and matrix phase (21.9% Ti–6.66% W–6.16% Mo–65.28% NiCo) are established [12]. Previously published data of other authors on the positive effect of WC, Cr_3C_2, and Mo_2C on the mechanical properties of bulk cermets [19] are confirmed in this study for plasma coatings as well. Using liquid-phase sintering at 1400°C for 1 h during the manufacture of the powder was positive, the annular zone was formed, and its volume increased the TiC content, which we did not observe earlier in the manufacture of the powder using solid-phase sintering at 1100°C [1].

In the initial powders for spraying and for coatings 1.2 and 2.2, the contribution of the hardness of carbides to the hardness of cermet under a load on the indenter of 20 G was calculated using the rule of mixtures. The calculated contribution of the hardness of carbides to the hardness of the cermet powder for spraying is higher than the calculated contribution of the hardness of carbide to the hardness of the coating and is close to the hardness of TiC (Table 4). In coating 1.2, the hardness of carbides is implemented to a lesser extent than in coating 2.2 likely because of the larger volume fraction of the matrix phase, with the displacement of carbides in the matrix under the action of the indenter at the time of hardness measurement (Table 4). Earlier, the dependence of the microhardness of cermet upon deformation of carbides under the action of an indenter was analyzed taking

into account the "adjacency" coefficient calculated from the number of contacts between carbides [24].

CONCLUSIONS

Bulk TiC-based cermets with additional WC and Cr_3C_2 carbides and Ni matrix alloyed with Cr, Mo, and 2.8 wt % C were used to fabricate powders for spraying of plasma coatings. The compositions of cerments provided the compensation of carbon losses at all stages of coating production and the formation of an annular zone, which determines the increase in the TiC content in the coatings by 20%.

The microhardness of cermet with an initial carbide content of 60 vol % is 15.26−16.83 GPa with a load on the indenter of 200 G and 20.91−24.68 GPa with a load on the indenter of 20 G. The difference in values was explained by the effect of the scale factor.

The contribution of the microhardness of carbides to the microhardness of cermet with the initial carbide content of 60 vol % is calculated according to the rule of mixtures based on their volume fraction and the microhardness of cermet at a load on the indenter of 20 G. In the initial powder prepared for spraying, this contribution has a high value of 33.19 GPa, close to the microhardness of TiC carbide. In the coating, the calculated contribution of the microhardness of carbides is lower—28.09 GPa.

REFERENCES

1. Kalita, V.I., Radyuk, A.A., Komlev, D.I., Ivannikov, A.Yu., Mikhailova, A.B., and Alpatov, A.V., Cermet plasma TiC–Cr_3C_2–NiCr–Mo–C coatings, *Inorg. Mater.: Appl. Res.*, 2019, vol. 10, no. 2, pp. 402−410.
https://doi.org/10.1134/S2075113319020205

2. Tolstobrov, A.K., Mitrofanov, B.V., and Zashlyapin, M.Yu., Effect of the binder metal on the strength and wear resistance of plasma coatings based on titanium and titanium-zirconium carbonitrides, *Powder Metall. Met. Ceram.*, 1992, vol. 31, pp. 948−952.
https://doi.org/10.1007/BF00797622

3. Podchernyaeva, I.A., Kisel', V.M., Evdokimenko, Yu.I., Lavrenko, V.A., and Pasichnyi, V.V., Investigation of a wear-and corrosion-resistant coating of the TiCN−Ni-alloy system, obtained by high-speed gas-flame spraying, *Powder Metall. Met. Ceram.*, 1999, vol. 38, pp. 358−361.
https://doi.org/10.1007/BF02676169

4. Tian, L.-H., Li, C.-X., Li, C.-J., and Yang, G.-J., Effect of dispersed TiC content on the microstructure and thermal expansion behavior of shrouded-plasma-

sprayed FeAl/TiC composite coatings, *J. Therm. Spray Technol.*, 2012, vol. 21, nos. 3−4, pp. 689−694.

5. Tsidulko, A.G., Rusanov, V.M., Bobrov, G.V., Dokukina, I.A., Timofeev, I.I., and Shaposhnikova, T.I., Loss of carbon during plasma-spraying of clad carbide powders, *Powder Metall. Met. Ceram.*, 1992, vol. 31, pp. 883−885.
https://doi.org/10.1007/BF00797515

6. Berger, L.-M., Application of hardmetals as thermal spray coatings, *Int. J. Refract. Met. Hard Mater.*, 2015, vol. 49, pp. 350−364.

7. Hussainova, I. and Antonov, M., Assessment of cermets performance in erosive media, *Int. J. Mater. Prod. Technol.*, 2007, vol. 28, no. 3/4, pp. 361−376.

8. Rödiger, O., Zur kenntnis des systems wolframkarbid—titankarbid—chromkarbid, *Metall*, 1953, vol. 7, pp. 967−969.

9. Jin, C., Onuoha, C.C., Farhat, Z.N., Kipouros, G.J., and Plucknett, K.P., Reciprocating wear behaviour of TiC-stainless steel cermets, *Tribol. Int.*, 2017, vol. 105, pp. 250−263.

10. Wana, W., Xiong, J., and Liang, M., Effects of secondary carbides on the microstructure, mechanical properties and erosive wear of Ti(CN)-based cermets, *Ceram. Int.*, 2017, vol. 43, pp. 944−952.

11. Zheng, Y., You, M., Xiong, W., Liu, W., and Wang, S., Effect of Cr$_3$C$_2$ on valence-electron structure and plasticity of rim phase in Ti(C,N)-based cermets, *J. Am. Ceram. Soc.*, 2004, vol. 87, no. 3, pp. 460−464.

12. Xiong, H., Li, Z., and Zhou, K., TiC whisker reinforced ultra-fine TiC-based cermets: Microstructure and mechanical properties, *Ceram. Int.*, 2016, vol. 42, pp. 6858−6867.

13. Yang, Q., Xiong, W., Zhang, M., Huang, B., and Chen, S., Microstructure and mechanical properties of Mo-free Ti(C,N)-based cermets with Ni−xCr binders, *J. Alloys Compd.*, 2015, vol. 636, pp. 270−274.

14. Zhou, W., Zheng, Y., Zhao, Y., Ma, Y., and Xiong, W., Microstructure characterization and mechanical properties of Ti(C,N)-based cermets with AlN addition, *Ceram. Int.*, 2015, vol. 41, pp. 5010−5016.

15. Zhang, Y., Zheng, Y., Zhong, J., Yuan, Q., and Wu, P., Effect of carbon content and cooling mode on the microstructure and properties of Ti(C,N)-based cermets, *Int. J. Refract. Met. Hard Mater.*, 2009, vol. 27, pp. 1009−1013.

16. Zhan, B., Liu, N., Jin, Z.-B., Li, Q.-L., and Shi, J.-G., Effect of VC/Cr$_3$C$_2$ on microstructure and mechanical properties of Ti(C,N)-based cermets, *Trans. Nonferrous Met. Soc. China*, 2012, vol. 22, pp. 1096−1105.

17. Zhang, W.N., Wang, H.Y., Wang, P.J., Zhang, J., He, L., and Jiang, Q.C., Effect of Cr content on the SHS reaction of Cr−Ti−C system, *J. Alloys Compd.*, 2008, vol. 465, pp. 127−131.

18. Wan, W., Xiong, J., Yang, M., Guo, Z., Dong, G., and Yi, C., Effects of Cr$_3$C$_2$ addition on the corrosion behavior of Ti(CN)-based cermets, *Int. J. Refract. Met. Hard Mater.*, 2012, vol. 31, pp. 179−186.

19. Manoj Kumar, B.V., Basuw, B., Kang, S., and Ramkumar, J., Erosion wear behavior of TiCN−Ni cermets containing secondary carbides (WC/NbC/TaC), *J. Am. Ceram. Soc.*, 2006, vol. 89, no. 12, pp. 3827−3831.
https://doi.org/10.1111/j.1551-2916.2006.01277.x

20. Pirso, J., Viljus, M., and Letunovitš, S., Friction and dry sliding wear behaviour of cermets, *Wear*, 2006, vol. 260, pp. 815−824.

21. Kiparisov, S.S., Levinskii, Yu.V., and Petrov, A.P., *Karbid titana. Poluchenie, svoistva, primenenie* (Titanium Carbide. Obtaining, Properties, Application), Moscow: Metallurgiya, 1987.

22. Kalita, V.I., Radyuk, A.A., Komlev, D.I., et al., Cermet plasma coatings based on silicon carbide, *Inorg. Mater.: Appl. Res.*, 2019, vol. 10, pp. 1145−1152.
https://doi.org/10.1134/S2075113319050095

23. Kalita, V.I. and Komlev, D.I., *Plazmennye pokrytiya s nanokristallicheskoi i amorfnoi strukturoi* (Plasma Coatings with Nanocrystalline and Amorphous Structure), Moscow: Biblioteka, 2008.

24. Grathwohl, G. and Warren, R., The effect of cobalt content on the microstructure of liquid-phase sintered TaC−Co alloys, *Mater. Sci. Eng.*, 1974, vol. 14, pp. 55−65.

Translated by L. Mosina